CHAPTER V

RESULTS AND DISCUSSION

In this chapter, the experimental results and discussion were described and divided into three major parts, namely, influence of mixed of Al_2O_3 and MgO to TiO_2 electrode layer, influence of sintering temperature and influence of double-layer structure of the thin film electrode on the performance of dye sensitized solar cell.

5.1 Effect of modification of TiO_2 electrode layer

5.1.1 Modification of TiO_2 electrode layer by adding Al_2O_3

TiO_2 electrode later was modified by addition of Al_2O_3 to electrode at the percentage of Al_2O_3/TiO_2 was 0.25 wt %, 1.0 wt % and 2.0 wt %, the electrode calcined at 400°C for 120 minutes and the number of coats were 500 coats have film thickness was approximately 10.5 μm which sinter temperature and the thickness gave highest the efficiency of dye sensitized solar cell, this work study influence of percentage of Al_2O_3/TiO_2 on performance of dye sensitized solar cell.

XRD patterns for the Al_2O_3/TiO_2 composite and bare TiO_2 are shown in Figure 5.1. It is apparent that the crystalline form of TiO_2 is anatase, rutile and brookite phase. It has been reported that anatase phase has higher photocatalytic oxidation-reduction activity than rutile phase. The band gap energies for anatase phase and rutile phase have been estimated to be 3.2 and 3.0 eV, respectively (Chen et al., 2010). The results from XRD showed that weight fraction of anatase phase increases when the mixing of Al_2O_3 increases (see in Table 5.1). The added alumina oxide role was based on the crystal growth inhibiter, which leading to small grain size correlated with high surface area (see in Table 5.1).

The amount of Al on Ti catalyst was determined using inductively coupled plasma atomic emission spectroscopy (ICP-AES). From ICP analysis the ratio of Al_2O_3/TiO_2 atomic ratio of Al_2O_3-TiO_2 mixed oxide calcined at 400°C for 120

minutes showed in Table 5.1. From result of ICP analysis found that the contents of Al less than the nominal value may because the preparation of mixed oxide sol.

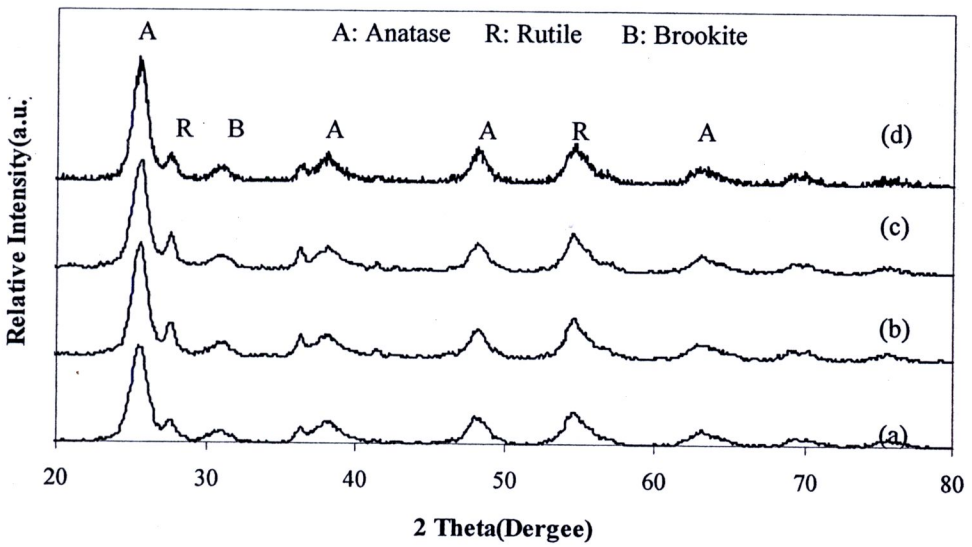

Figure 5.1 XRD patterns of Al_2O_3/TiO_2 powders at various percentages of Al_2O_3/TiO_2 (a) 0 wt %, (b) 0.25 wt %, (c) 1.0 wt % and (d) 2.0 wt %

Table 5.1 Crystal size, surface area and weight fraction of anatase, rutile and brookite of Al_2O_3/TiO_2 powders calcined at 400°C for 120 minutes

Al_2O_3/TiO_2 (wt %)	Crystallite size (nm)	Surface area (m^2/g)	Amount of Al from ICP (wt %)	W_A	W_R	W_B
0	7.80	80.60	-	0.62	0.19	0.18
0.25	6.90	96.10	0.16	0.70	0.15	0.15
1.0	6.80	99.80	0.83	0.70	0.13	0.17
2.0	6.10	105.70	1.77	0.73	0.12	0.15

W_A : weight fraction of anatase phase

W_R : weight fraction of rutile phase

W_B : weight fraction of brookite phase

That surface is more basic than bare TiO_2, the higher basicity of surface favors dye attachment through its carboxylic acid groups which can cause the increase of absorbed dye amount (Wu et al., 2008, Yang et al., 2009). Therefore, an increase in dye adsorption is expected. Formation of dye agglomerates mainly hinges on to the high acidity nature of the carboxylic groups of the dye or pH of electrolytic composition or surface chemical property of material. The isoelectric point (IEP) of material is the pH at which the materials surface carries no net electrical charge. At a pH below the isoelectric point (IEP), metal oxide surface carries a net positive charge, and above the pH, the negative charge predominates. The isoelectric point (IEP) is therefore an important parameter by which the difference in injection efficiency at the metal oxide|dye interface could also be arisen because it determines the stability of the dye.

Figure 5.2 and Table 5.2 presents the isoelectric point (IEP) values of TiO_2 and Al_2O_3/TiO_2 electrode. It is evident that the isoelectric point (IEP) of all mixing Al_2O_3 electrode are some higher than that of the pure TiO_2 electrode. So when adsorbed with N3, the absorbance of the Al_2O_3/TiO_2 electrode is enhanced compared with that of the TiO_2 electrode, showing that the modification of Al_2O_3 apparently increases the amount of adsorbed dye molecules (show in Figure 5.3). The higher amount of dye molecules is attributed to the higher basicity of the TiO_2 electrode upon Al_2O_3 modification. It has been observed that the carboxyl groups in the N3 dye molecules are more easily adsorbed to the surface of the layers if the modification materials are more basic than TiO_2 (Jung et al., 2005).

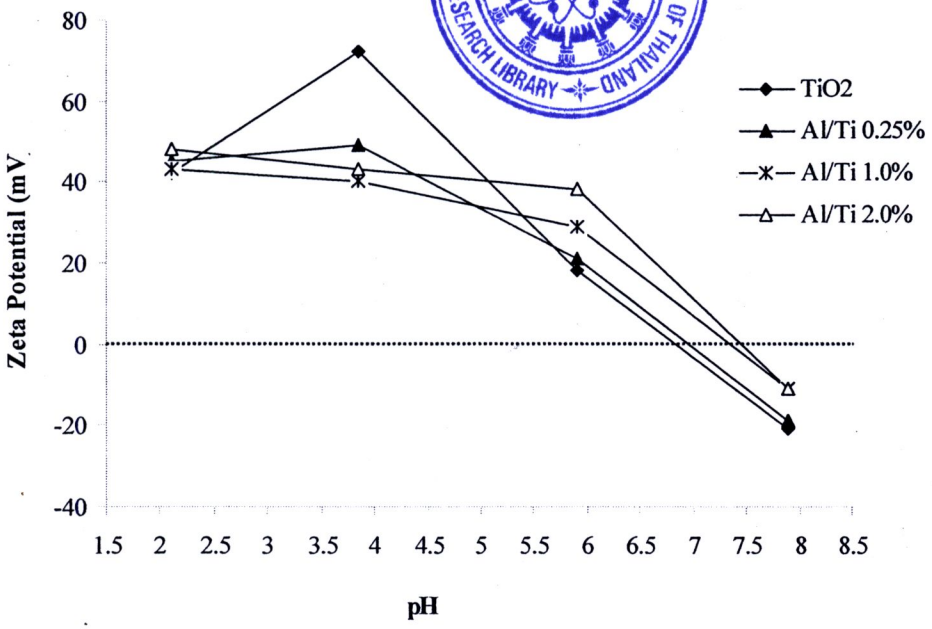

Figure 5.2 Isoelectric point (IEP) of TiO_2 modified with various Al_2O_3 contents

Table 5.2 The isoelectric point (IEP) of TiO_2 and Al_2O_3/TiO_2 at various percentage of Al_2O_3/TiO_2

Al_2O_3/TiO_2 (wt %)	Isoelectric point (IEP)
0	6.69
0.25	6.81
1.0	7.20
2.0	7.33

Quantitative analysis was done by desorbed dye molecules from presoaked TiO_2 and Al_2O_3/TiO_2 film into a solution of 0.1 M NaOH in ethanol (1:1 in volume fraction) and measuring its absorption spectrum. The amount of the adsorbed dye on TiO_2 and Al_2O_3/TiO_2 was also showed in Figure 5.3.

Figure 5.3 shows the UV–visible absorption spectra for N3 dye absorbed TiO_2 and Al_2O_3/TiO_2 electrodes. The wavelength of laser was selected as 510 nm because the dye molecules have maximum absorption around this wavelength. It can be

concluded that absorption is enhanced with increasing the contents of Al_2O_3 modification. The increased absorption led to enhanced light harvesting and thereby increased short circuit photocurrent (current density) for the corresponding DSSC. It is assumed that the Al_2O_3/TiO_2 layer can also adsorb the dye, which absorbs the light and generates excited states of the dye.

Figure 5.4 shows the FT-IR spectra of modified TiO_2 with the different of Al_2O_3 contents. The 1600 and 1380 cm^{-1} peaks were attributed to the asymmetric and symmetric stretching vibrations of $-COO^-$ group (Luo et al., 2008), and their intensity increased with mixing Al up to 1 wt %. Table 5.3 shows the amount of functional groups of carboxylic acid, obtained by calculating the area under the graph of the functional groups divided by the surface area. Both UV-vis and FT-IR spectra data support the finding that the carboxylate acid in N3-TiO_2 after Al_2O_3 addition. After adding Al to 2 wt % the results are shown carboxylate acid on the surface decrease and the amount of dye absorption decreased. These results clearly indicate that N3 should also adsorb on TiO_2 powder surfaces via its carboxylate form. Besides, although a large number of the carboxyl groups in the dye sensitizer will increase the electron transfer efficiency due to their better anchoring to the TiO_2 surface (Chen et al., 2010).

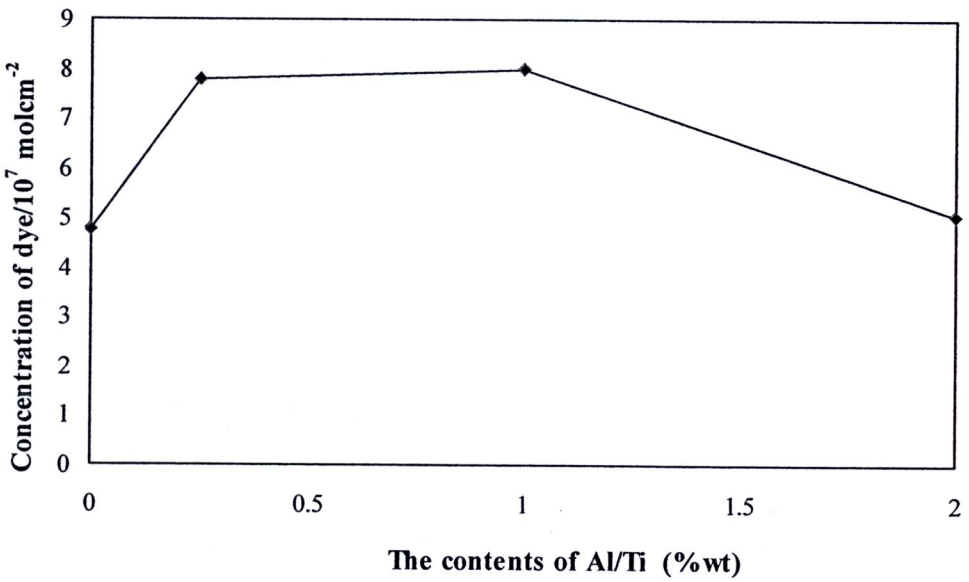

Figure 5.3 Relationship between concentrations of dye with various contents of Al_2O_3/TiO_2

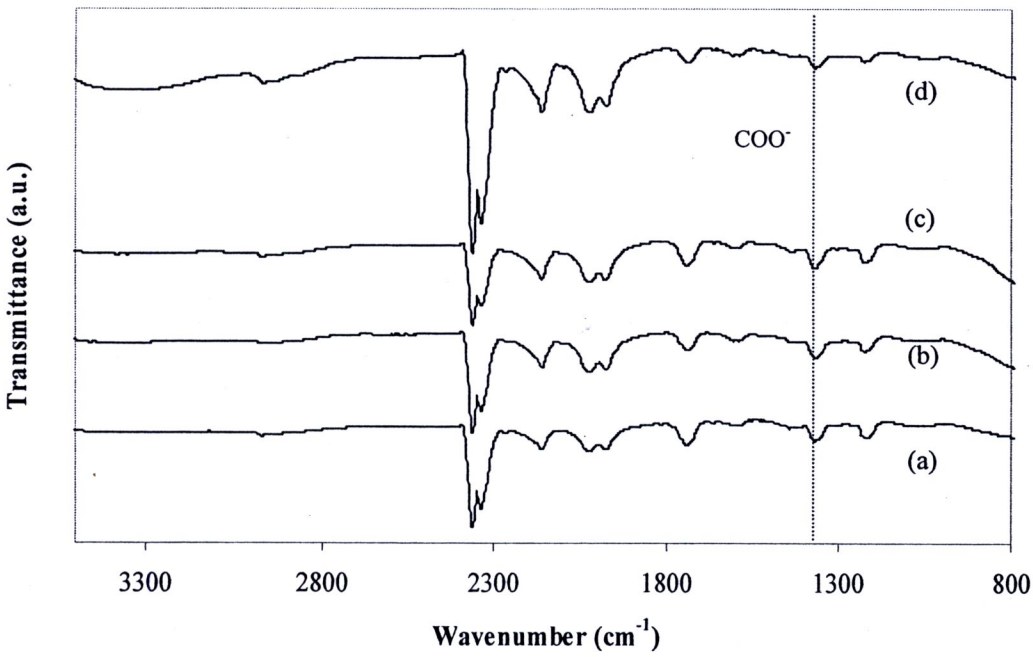

Figure 5.4 FTIR spectra of modified TiO_2 with various Al_2O_3 contents (a) 0 wt %, (b) 0.25 wt %, (c) 1.0 wt % and (d) 2.0 wt %

Table 5.3 The quantity of carboxylate acid group on surface of TiO_2 and Al_2O_3/TiO_2 at various percentage of Al/Ti

Al_2O_3/TiO_2 (wt %)	Weight (g)	Surface area (m^2/g)	Area peak of COO^-	Surface area×Weight = Surface total	Area peak of COO^- per Surface total
TiO_2	0.001	80.60	113.78	0.08	1411.70
0.25	0.001	96.10	161.74	0.10	1683.10
1.0	0.001	99.80	173.47	0.99	1738.20
2.0	0.0013	105.70	91.15	0.14	663.30

The overall view of the efficiency of cells fabricated from bare TiO_2 and Al_2O_3/TiO_2 electrodes under 100 $mW \cdot cm^{-2}$illumination. The corresponding solar cell

parameters are summarized in Table 5.4. When the contents of Al_2O_3 is mixed for less than 2.0 wt % a higher short circuit current, open circuit photo-voltage and conversion efficiency with increased the contents of Al_2O_3 can be observed for the electrodes. The cell showed great improvement in the cell parameters when the contents of Al indicated that 1.0 wt % of Al_2O_3/TiO_2 electrode. The current density increased from 6.89±1.4 to 7.85±0.9 $mA \cdot cm^{-2}$, and the voltage from 0.60±0.1 to 0.80±0.04 volt. The cell conversion efficiency increased from 3.50±0.2% to 5.04±0.2 %, showing the positive role of the Al_2O_3 mixing on TiO_2. When the mixing Al was increased to 2.0 wt %, the amount of the dye adsorbed shows decrease with the increase of Al_2O_3 content, which will result in the decrease of the light harvesting efficiency. Upon further increase of mixing the contents of Al_2O_3, the conversion efficiency drastically decreased along with other cell parameters. From the poor conversion efficiencies, it can be inferred that excessive Al_2O_3 beyond tunneling distance plays a negative role in the photoelectron conversion process (Wu et al., 2008)

Table 5.4 Electrochemical properties of dye sensitized solar cell of Al_2O_3/TiO_2 electrode calcined at 400°C with 500 coats

Al_2O_3/TiO_2 (wt %)	V_{oc} (Volt)	J_{sc} ($mA \cdot cm^{-2}$)	Fill Factor	Efficiency (%)
0	0.60±0.1	6.89±1.4	0.89±0.3	3.50±0.2
0.25	0.73±0.01	7.74±0.3	0.71±0.01	4.01±0.08
1.0	0.80±0.04	7.85±0.9	0.81±0.1	5.04±0.2
2.0	0.76±0.01	4.53±0.4	1.00±0.06	3.45±0.09

5.1.2 Modification of TiO_2 electrode layer by adding MgO

TiO_2 electrode layer was modified by addition of MgO to TiO_2 electrode at the percentage of Mg/Ti was 0.25%, 1.0% and 2.0% (wt %), the electrode calcined at 400°C for 120 minutes.

The phase structure of the films was examined by XRD. Figure 5.5 show the XRD pattern of the bare TiO_2 and the MgO/TiO_2 composite. The peaks are very sharp implying that the TiO_2 films were well crystallized (Bihui et al., 2010). The XRD pattern of the MgO/TiO_2 composite is found to be similar as that of bare TiO_2. Table 5.5 indicated that the additions of magnesium inhibited the anatase phase increase slightly.

Table 5.5 reported the various contents of Mg on Ti catalyst from ICP analysis. From result of ICP analysis found that the contents of Mg less than the nominal value may because the preparation of mixed oxide sol. Besides, this table showed that the crystallite size and surface area which the MgO/TiO_2 had higher surface area than pure TiO_2.

Generally, for a given dye, the amount of dye adsorbed on TiO_2 and MgO/TiO_2 is correlated with the specific area of TiO_2 and MgO/TiO_2. The amount of the adsorbed dye on TiO_2 and MgO/TiO_2 was also showed in Figure 5.7. It can be observed that the amount of the adsorbed dye decreases with the increase of the MgO content, while its specific surface area increase compared to that of unmodified TiO_2 (see in Table 5.5). So the specific surface area was not mainly responsible for the decrease of the dye adsorption.

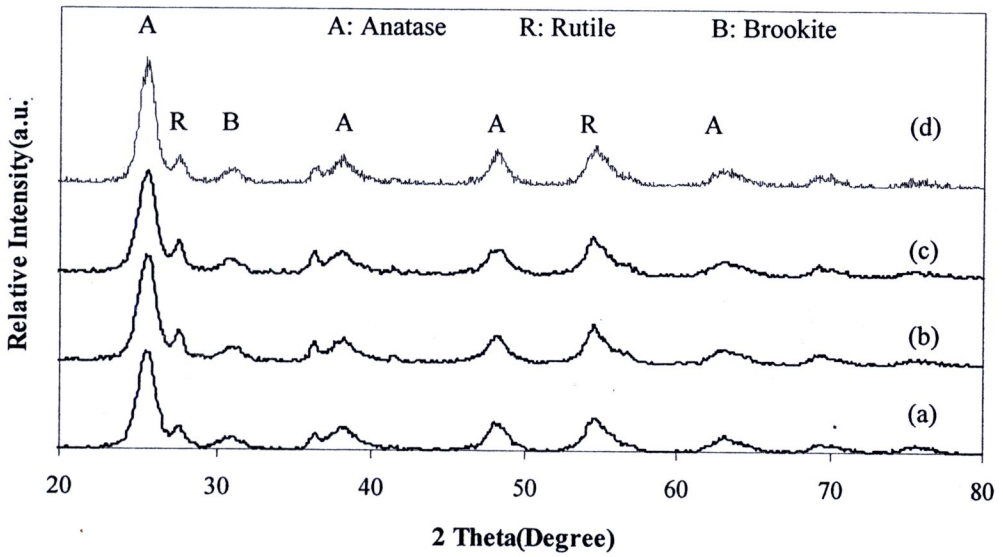

Figure 5.5 XRD patterns of MgO/TiO_2 powders at various percentage of Mg/Ti (a) 0 wt %, (b) 0.25 wt %, (c) 1.0 wt % and (d) 2.0 wt %

Table 5.5 Crystal size, surface area and weight fraction of anatase, rutile and brookite of MgO/TiO_2 powder calcined at 400°C for 120 minutes

MgO/TiO_2 (wt %)	Crystallite size (nm)	Surface area (m^2/g)	Amount of Al from ICP (%wt)	W_A	W_R	W_B
0	7.80	80.60	-	0.62	0.19	0.18
0.25	6.40	94.60	0.22	0.70	0.13	0.17
1.0	6.90	90.80	0.42	0.70	0.12	0.17
2.0	7.30	88.50	1.89	0.71	0.13	0.16

In order to clarify the reason that a less dye uptake was obtained for MgO modified TiO_2, zeta potentials of the TiO_2 particles modified with various MgO contents were measured. Figure 5.6 shows the zeta potential of TiO_2 modified with various MgO contents and Table 5.6 presents the isoelectric point (IEP) values of TiO_2 and MgO/TiO_2 electrode. The results show a clear difference in isoelectric point (IEP) between the samples. It can be clearly observed that the isoelectric point (IEP) of the particles shifts to lower pH values with the increase of MgO content. For a

given curve, when independent variable of pH is less than the isoelectric point (IEP) of TiO_2, the zeta potential for the sample is low the horizontal axis, which means that the surface of MgO/TiO_2 nanopareicles is the higher acidcity of surface, which is adverse to the adsorption of dye molecules onto TiO_2 surface (Cheng et al., 2008). So the isoelectric point (IEP) is responsible for the decrease of the dye adsorption for MgO modified TiO_2.

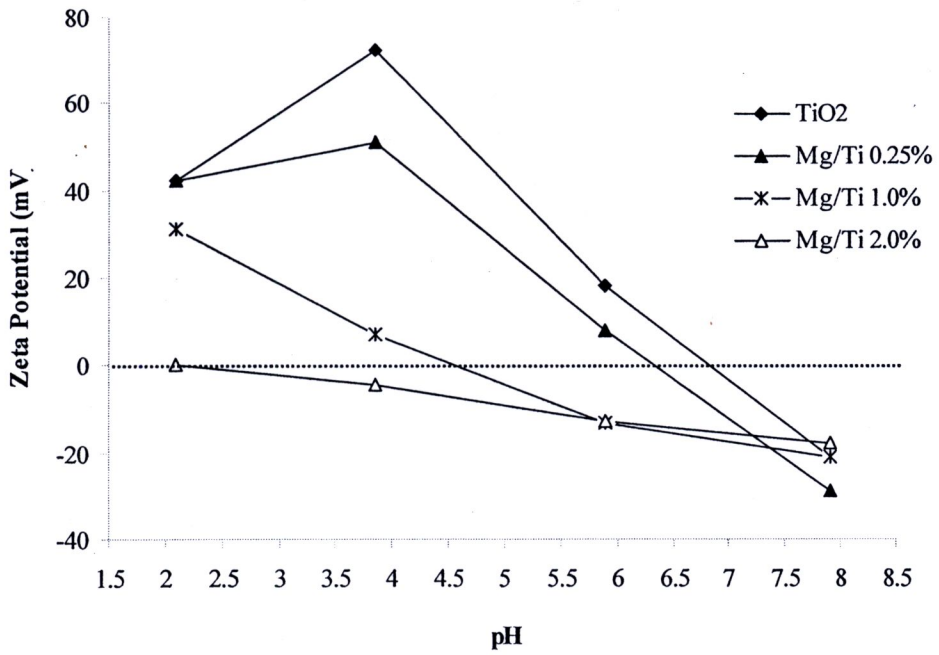

Figure 5.6 Zeta potentials of TiO_2 modified with various MgO contents

Table 5.6 The isoelectric point (IEP) of TiO_2 and MgO/TiO_2 at various percentage of Mg/Ti

MgO/TiO_2 (wt %)	Isoelectric point (IEP)
0	6.69
0.25	6.30
1.0	4.55
2.0	0.63

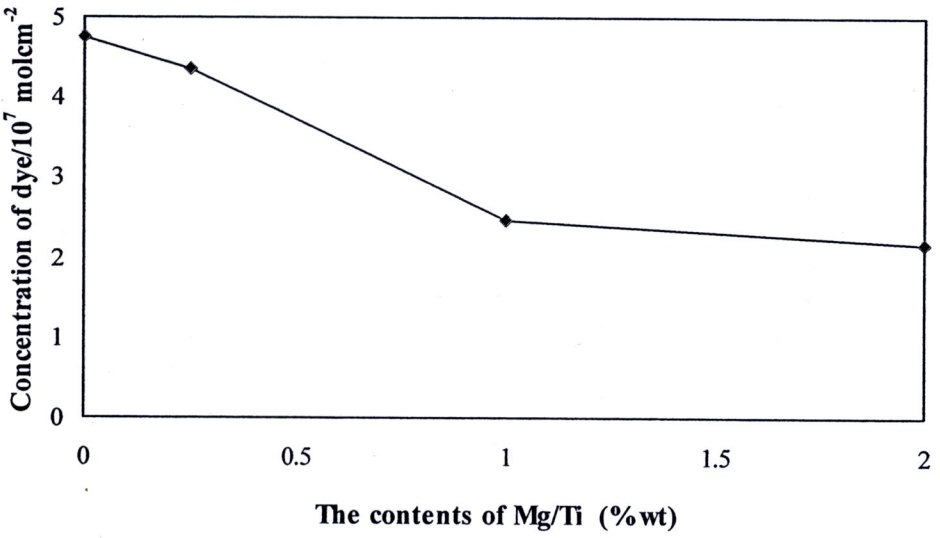

Figure 5.7 Relationship between concentrations of dye with various contents of MgO/TiO_2

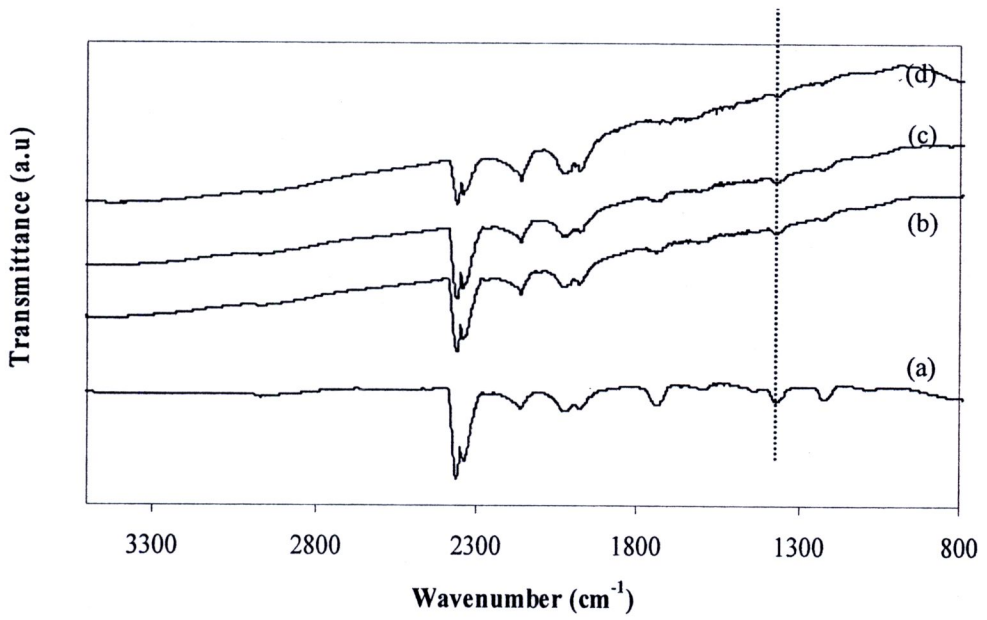

Figure 5.8 FTIR spectra of modified TiO_2 with various MgO contents (a) 0 wt %, (b) 0.25 wt %, (c) 1.0 wt % and (d) 2.0 wt %

If considered carboxylate acid on the surface of TiO_2 after improve. FT-IR results showed that the position wavenumber 1380 cm^{-1} was attributed to the symmetric stretching vibrations of $-COO^-$ group was decreased when the amount of Mg increased. This means that among the adhesive surface is less. Consistent with the results of dye absorption (show in Figure 5.7 and Table 5.7), the amount of dye absorption is reduced. This is because the carboxylic acid group in the dye reacted more favourably on a surface with a more basic nature or higher the isoelectric point (IEP), as show in Table 5.6 (Ganapathy et al., 2010).

The photovoltaic parameters of DSSC of MgO/TiO_2 electrode calcined at 400°C at various the amount of Mg are summarized in Table 5.8. The inset shows the corresponding photocurrent density (J_{SC}) of DSSC. The photocurrent density decreases as a function of MgO content, which confirmed the previous discussion about the dye adsorption effect of MgO modification. So, the overall efficiency of cell was decease after added Mg on Ti sol.

Table 5.7 The quantity of Carboxylate acid group on surface of TiO_2 and MgO/TiO_2 at various percentage of MgO

MgO/TiO_2 (wt %)	Weight (g)	Surface area (m^2/g)	Area peak of COO^-	Surface area×Weight = Surface total	Area peak of COO^- per Surface total
TiO_2	0.001	80.60	113.78	0.08	1411.70
0.25	0.002	94.60	111.97	0.19	591.83
1.0	0.0016	90.80	76.73	0.15	528.06
2.0	0.0013	88.50	64.80	0.12	563.21

Table 5.8 Electrochemical properties of dye sensitized solar cell of MgO/TiO_2 electrode calcined at 400°C with 500 coats

MgO/TiO_2 (wt %)	V_{oc} (Volt)	J_{sc} ($mA \cdot cm^{-2}$)	Fill Factor	Efficiency (%)
0	0.60±0.1	6.89±1.4	0.89±0.3	3.50±0.2
0.25	0.77±0.06	4.90±0.8	0.75±0.1	2.79±0.07
1.0	0.74±0.02	3.79±0.6	0.82±0.1	2.27±0.09
2.0	0.60±0.04	1.32±0.2	0.52±0.05	0.41±0.05

5.2 Effect of calcinations temperature on mixed oxide electrode layer

Al_2O_3/TiO_2 (1.0 wt %) sol was prepared via sol-gel method. It has been used as a working electrode in DSSC. In general, sintering temperature affect on photocurrent-voltage characteristic because of the change of crystallite size, surface area and phase transformation of TiO_2 (Ngamsinlapasathian et al., 2005). In this study, the sintering temperature was varied to be 300°C, 400°C and 500°C.

The crystalline nature of the TiO_2 particles was investigated using XRD and the results are shown in Figure 5.9. X-ray diffraction analyses show the presence of anatase structure al low temperature. Fraction of rutile phase is detected with increasing the calcinations temperature 500°C.

Crystalline size of the particles was estimated from the full width at half maximum (FWHM) of the intense (1 0 1) diffraction peak of anatase phase according to the Scherrer's equation. The primary particle sizes of TiO_2 particle using Scherrer's equation are listed in Table 5.9. The estimated sizes were 5.2 nm, 7.0 nm and 8.2 nm for sintered temperature at 300°C, 400°C and 500°C, respectively. When the higher temperature, the smaller the BET surface area of the sample. It was also found that the

crystalline size, surface area and phase transformation were affected by the calcinations temperatures.

The increasing of particle size can be attributed of crystallization of the surface amorphous structure and the connection of those small nanoparticles at higher calcined temperature are important for help electron transport of TiO_2 film electrode (Zhao et al., 2008).

Han et al., 2005 have reported that a DSSC with 71% anatase (and remaining rutile) in its film has shown a larger conversion efficiency of 6.8% compared to 5.3% of a cell with pure anatase TiO_2. Conpared with anatase, rutile TiO_2 has superios light scattering properties because of its higher refraction index and is chemically more stable and potentrally cheaper to produce. Higher light scattering properties are beneficial from the perspectives of effective light harvesting.

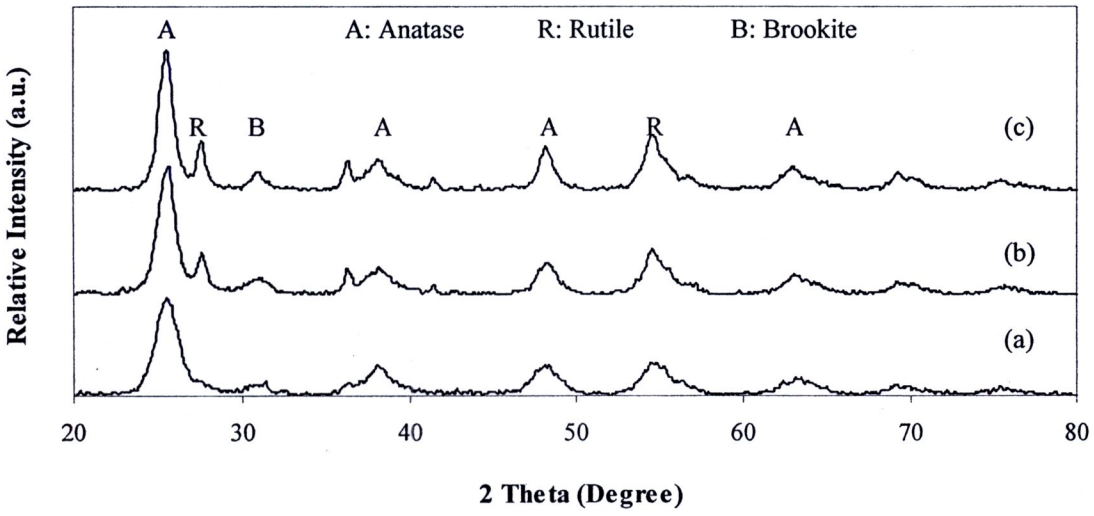

Figure 5.9 XRD patterns of 1.0% (wt %) of Al_2O_3/TiO_2 powders sintered at different temperature for 120 minutes, (a) 300°C, (b) 400°C and (c) 500°C

Table 5.9 Crystal size, surface area and weight fraction of anatase and rutile phase of 1.0 wt % of Al_2O_3/TiO_2 powders at different temperature for 120 minutes

Calcined temperature of 1.0 wt % (°C)	Crystallite size (nm)	Surface area (m^2/g)	W_A	W_R	W_B
300	5.20	134.40	0.85	0.04	0.1
400	7.00	99.20	0.70	0.13	0.17
500	8.20	66.90	0.66	0.20	0.14

W_A : weight fraction of anatase phase

W_R : weight fraction of rutile phase

W_B : weight fraction of brookite phase

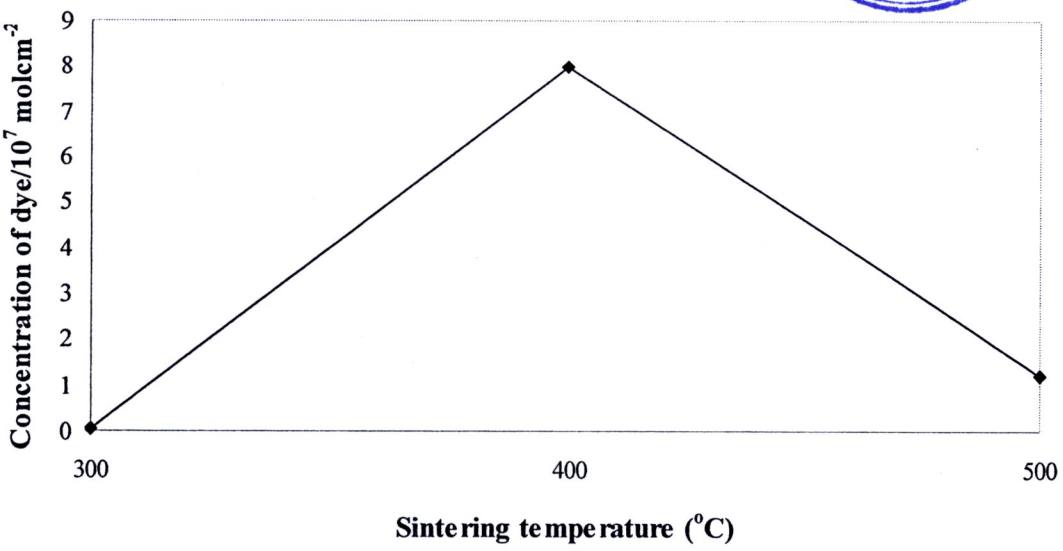

Figure 5.10 Relationship between concentrations of dye and sintering temperatures with 500 coats of 1.0 wt % of Al_2O_3/TiO_2 for 120 minutes

The resulting of electrochemical properties in Table 5.10 of the thickness of TiO_2 was about 10.5 μm at various sintering temperature for 120 minutes indicated that sintering temperature influence on performance of DSSC, this table ware show short-circuit current (Jsc), open-circuit voltage (Voc), fill factor (FF) and efficiency of DSSC.

The photocurrent characteristic (Jsc) increases maximal up to 400°C and it decreases with increases in sintering temperature. Although surface area of the cell calcined at 400°C less than the cell calcined at 300°C, in contrast the amount of dye adsorption of electrode sintered at 400°C higher than the electrode sintered at 300°C. In general, the amount of adsorbed dye increases related with number of inject electron in metal electrode leading to an increase of Jsc. Hence, the electrode was calcined at 400°C improve the connection between particles which help electron transport of TiO_2 film electrode.

The efficiency of the cell sintered at 500°C decreases was show Table 5.10 because of the increasing of rutile phase was show in Table 5.9 leading to large particle size, less of surface area which due to absorption of dye not enough. Beside, it is well known that electron diffusion coefficient (Dn) for the rutile film is about one order of magnitude lower than that of the anatase film, implying that electron transport is slower in the rutile layer than in the anatase layer (Park et al., 2010), it cause current density decreases with the performance of dye sensitized decreases.

Table 5.10 Electrochemical properties of dye sensitized solar cell of 1.0 wt % of Al_2O_3/TiO_2 electrode calcined at various temperatures for 120 minutes, the thickness of Al_2O_3/TiO_2 film about 10.5 μm

Sintering temperature of Al_2O_3/TiO_2 (1.0 wt %), (°C)	V_{oc} (Volt)	J_{sc} ($mA \cdot cm^{-2}$)	Fill Factor	Efficiency (%)
300	0.59±0.005	1.90±0.5	0.49±0.07	0.54±0.1
400	0.80±0.04	7.85±0.9	0.81±0.1	5.04±0.2
500	0.74±0.01	5.51±0.3	1.01±0.04	4.16±0.14

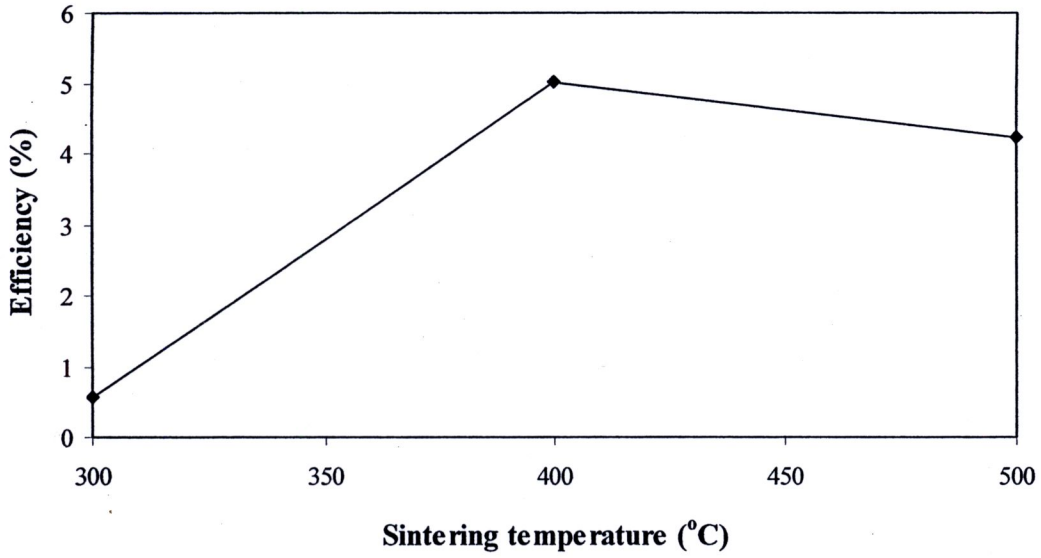

Figure 5.11 The efficiency of 1.0% (wt %) of Al_2O_3/TiO_2 at different calcined temperatures for 120 minutes

5.3 Dye-sensitized solar cell using double-layered conducting glass

TiO_2 electrode was deposited onto conducting glass by the layer-by-layer deposition of double-layered TiO_2 particles. The layer was coated on conducting glasses by using the ultrasonic spray coater, number of coats constant at 500. After deposition, thin film was dried by a hair dryer and then sintered at 400°C. It is expected that the double layer film electrode can be extended to other composite films with different layer structures and morphologies for enhancing the efficiencies of DSSC.

Type A: Deposition Al_2O_3/TiO_2 1.0 wt % sol on a conducting glass, calcined at 400°C for 120 minutes and the number of coats were 500 coats have film thickness was approximately 10.5 μm which sinter temperature, the thickness and the percentage of Al gave highest the efficiency of dye sensitized solar cell.

Type B: Deposition pure TiO_2 sol on a conducting glass and the number of coats were 250 coats and then sintered at 400°C for 120 minutes. Next, the deposition process of the mixed oxide electrode Al_2O_3/TiO_2 1.0 wt % was to obtain the desired

film thickness same single-layer electrode. The electrode was finally sintered at a temperature 400°C for 30 minutes.

After the above heat treatment procedure, the resulting TiO_2 electrodes were soaked in an ethanol solution containing 0.5mM N3 dye at room temperature for 12 hour. Then the electrodes were sequentially washed with ethanol and dried. In order to analyze the loading amount of dye in TiO_2 electrode, the dye was desorbed from TiO_2 electrode into NaOH solution in ethanol. The UV-vis spectrophotometer was employed to measure the dye concentration of the desorbed dye solution. The UV-vis spectrum showing the adsorbent of wavelength for TiO_2 electrode can be observed to have the absorption feature. Table 5.11 shows the comparison of concentration of dye value between a single layered and double layered electrode structure. The adsorption of dye in single layered and double layered are 7.9725×10^{-7} mol·cm^{-2} and 8.5048×10^{-7} mol·cm^{-2}, respectively. Consequently, it can be confirmed that the conjugation status exists between dye and the thin film electrode, and multiple layered organization will affect photoelectrical electrode production. When compared with single layered and double layer thin film result the prepared double layer thin film with a good compactness can increase the dye adsorption capability of the thin film and enhance its adsorption percentage. These dyes should incorporate functional groups (interlocking groups) as for example carboxylates or chelating groups, which besides bonding to the titanium dioxide surface, also effect an enhanced electronic coupling of the sensitizer with the conduction band of the semiconductor. The carboxylates groups serve to attach the Ru complex to the surface of the oxide and to establish good electronic coupling between the π^* orbital of the electronically excited complex (Gratzel et al., 2003, Nazeeruddin et al., 1993).

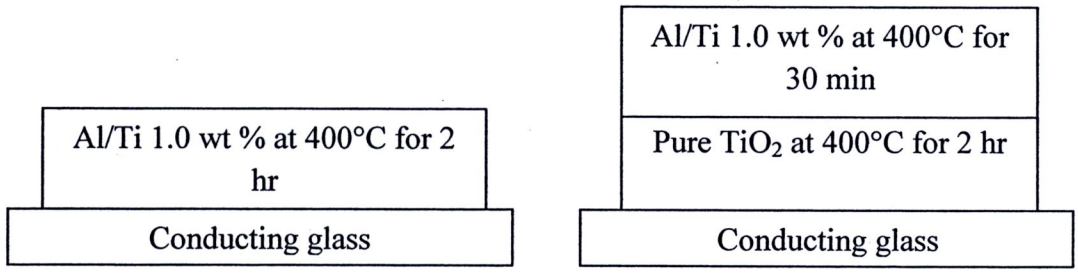

(a) (b)

Figure 5.12 Type of the mixed oxide electrode on conducting glass prepared for DSSC (a) Single-layer and (b) Double-layers

Table 5.11 The specific surface area of TiO_2 powders calcined at various temperatures

	Calcined temperature (°C)	Crystallite size (nm)	Surface area (m^2/g)	Concentration of dye ($mol \cdot cm^{-2}$)
Single-layer :				
Al_2O_3/TiO_2 1.0 wt %	400°C 120 min	6.95	99.20	7.97×10^{-7}
Double-layers :				
Pure TiO_2 (underlayer)	400°C 120 min	7.80	80.60	8.50×10^{-7}
Al_2O_3/TiO_2 1.0 wt % (overlayer)	400°C 30 min	5.69	120.20	

Figure 5.13 represents the diffused reflection spectra of single-layered and double-layer TiO_2 electrode. The diffused reflectance of the films increases as the scattering layers were added.

Table 5.12 compared the properties and photovoltaic parameters of single layered and double layered thin film electrode at nearly specific surface area, in which the thickness of single-layered electrode was experimentally controlled to be identical to that of double-layered electrode (ca. 10.5μm). As a result, from many dye

molecules are adsorbed on the surface of modification TiO_2 film structure, increases the photocurrent value (J_{SC}) from 7.85±0.9 to 8.74±0.9 $mA \cdot cm^{-2}$ and the photoelectrochemical properties of the double layer structure were improved and the overall energy conversion efficiency η was enhanced from 5.04±0.2% to 5.50±0.5%.

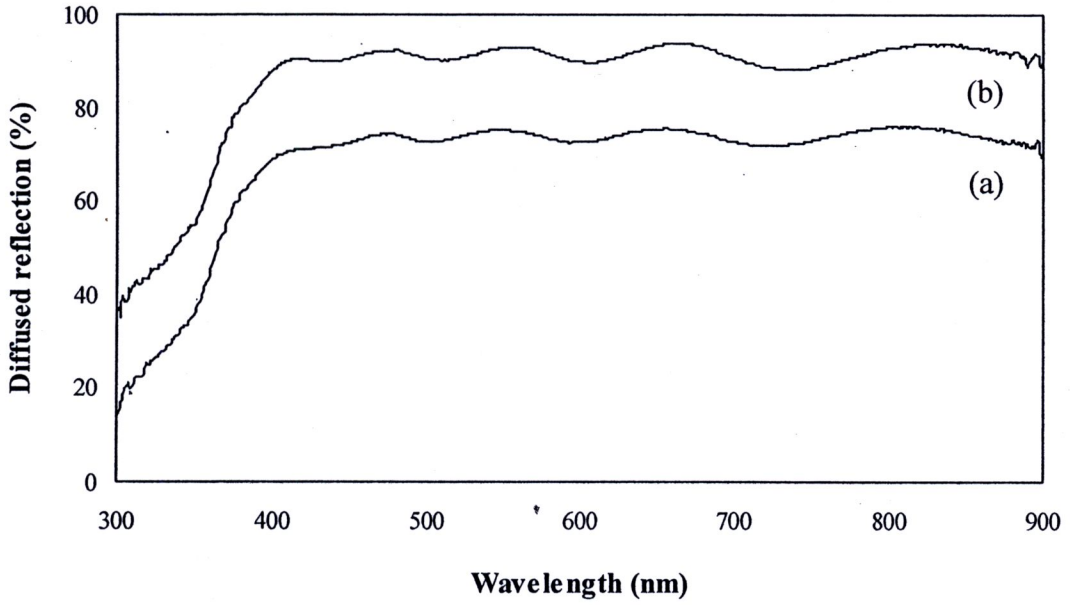

Figure 5.13 Diffused reflection of single-layered and double-layered (a) Single-layer and (b) Double-layer

Table 5.12 DSSC performance of single and double layers electrode

	V_{oc} (volt)	J_{sc} ($mA \cdot cm^{-2}$)	Fill Factor	Efficiency (%)
Single-layer : Al_2O_3/TiO_2 1.0 wt %	0.80±0.04	7.85±0.9	0.81±0.1	5.04±0.2
Double-layers : Pure TiO_2 (under) Al_2O_3/TiO_2 1.0 wt % (over)	0.73±0.005	8.74±0.9	0.86±0.03	5.50±0.5